Electronic Supplementary Material (ESI) for RSC Advances.

Electronic Supplementary Information

A "Turn-On" fluorescent probe for sensitive and selective detection of fluoride ions based on aggregation-induced emission

Man Du, Baolong Huo, Mengwen Li, Ao Shen, Xue Bai, Yaru Lai, Jiemin Liu*, Yunxu Yang*

Department of Chemistry and Chemical Engineering, School of Chemistry and Biological Engineering, University of Science and Technology Beijing, Beijing 100083, China

Corresponding Author: Yunxu Yang, Jiemin Liu

E-mail addresses: yxyang@ustb.edu.cn (Yunxu Yang);

liujm@ustb.edu.cn (Jiemin Liu)

Contents:

Table S1. Comparisons of proposed method with recently reported strategies for F^- detection.

Literature	Mechanism	Fluorophore	Wavelength/nm	Detection limit	Dynamic range	Response time
[1]	P-O cleavage	Dichlorofluorescein	λ_{ex} = 510 nm, λ_{em} = 536 nm	9.8 nM	—	10 min
[2]	Formation of hydrogen bonds with F^-	1,8-Naphalimide and Benzothizazole	λ_{ex} = 415 nm	0.41μM	—	10 s
[3]	AIE	Tetraphenylethene	λ_{em} = 560 nm	6×10^{-4} M	—	2 min
[4]	Si-O cleavage	Luciferin	—	1 μM	0 to 100 μM	—
[5]	Si-O cleavage	7-Diethylaminocoumarin	λ_{ex} = 490 nm	1.2×10^{-8} M	0 to 4 × 10^{-5} M	—
[6]	Si-C cleavage	BODIPYs	λ_{em} = 614-687 nm	14.9-92.7 nM	—	20-40 min
[7]	Si -O cleavage	7-Hydroxycoumarin	λ_{ex} = 375 nm	0.285 μM	0 to 60 μM	—
[8]	Lewis acid anion receptors	Naphthalene diimide	λ_{ex1} = 475 nm, λ_{em1} = 545 nm λ_{ex2} = 362 nm, λ_{em2} = 530 nm	17 μM; 18 μM	0 to 400 μM; 0 to 230 μM	—
[9]	Deprotonation of the N-H proton	1,8-Naphthalimide	λ_{ex} = 460 nm, λ_{em} = 525 nm	1.8 μM	0 to 23.3 μM	—
[10]	Si-O cleavage	Naphthalimide	λ_{ex} = 430 nm, λ_{em} = 550 nm	5.27 μM	0 to 160 μM	50 s
[11]	Si-O cleavage	Spiropyran	—	8.3×10^{-8} M	5.0×10^{-8} to 1.0×10^{-8} μM	30 min
[12]	Deprotonation	Benzimidazole	λ_{ex} = 425 nm, λ_{em1} = 510 nm, λ_{em2} = 592 nm	3.45×10^{-10} M	—	1 min
[13]	Breakage of the B-O bonds	QDs	λ_{ex} = 350 nm, λ_{em} = 625 nm	0.4 μM	0.4 to 2.8 μM	—
Our work	P-O cleavage AIE	HBT	λ_{ex} = 335 nm, λ_{em} = 470 nm	3.8 nM	0.5 to 10 μM	2 min

"—" Not mentioned.

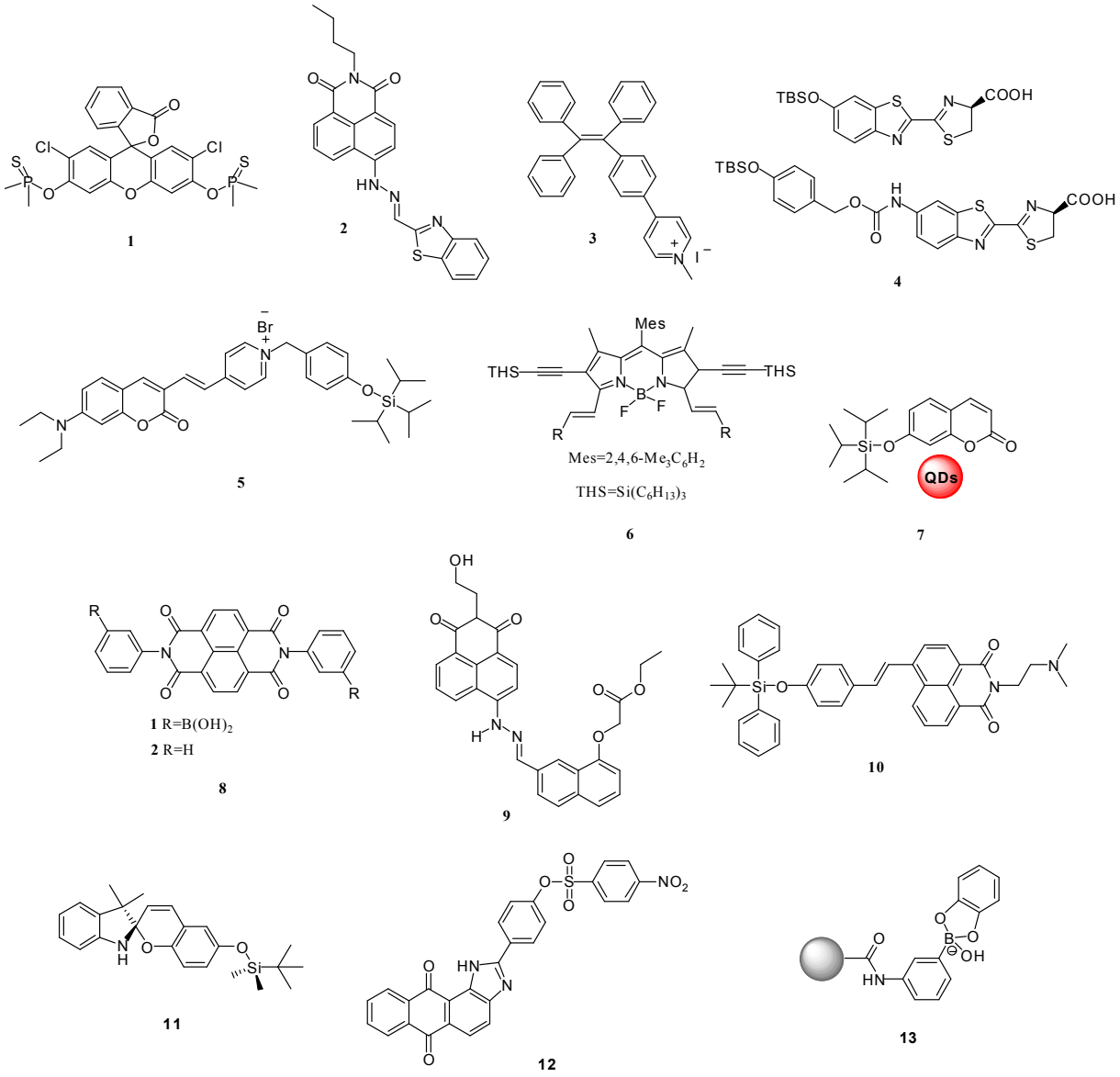

Fig. S1. Structures of probes recently reported for F^- detection.

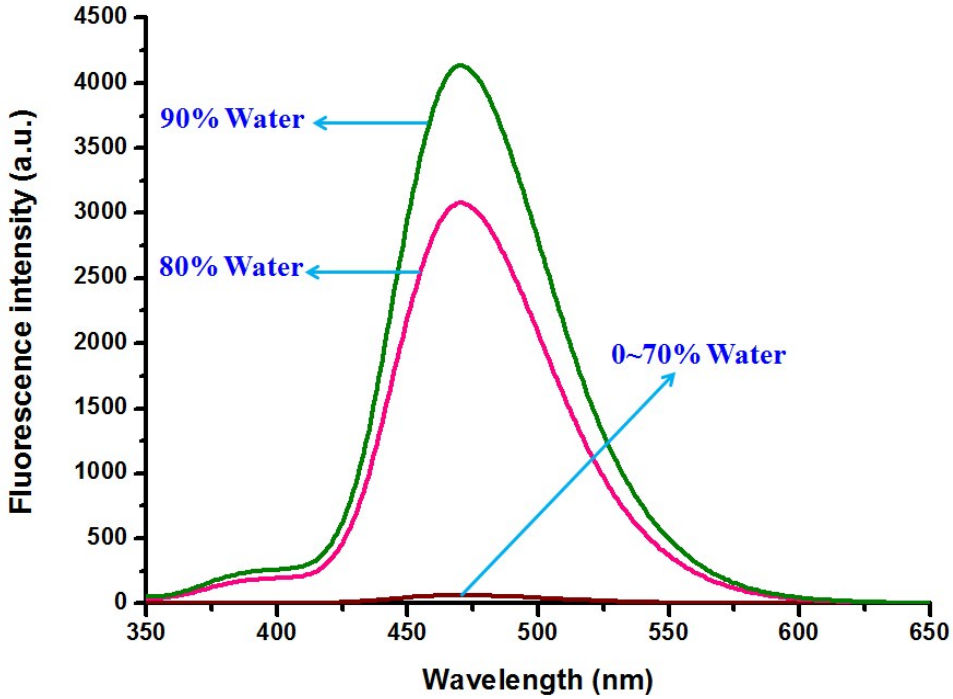

Fig. S2. Fluorescent spectra of **HBT** (10 μM) in the THF / H_2O mixture at different water fractions, λ_{ex}=335 nm, λ_{em}=470 nm.

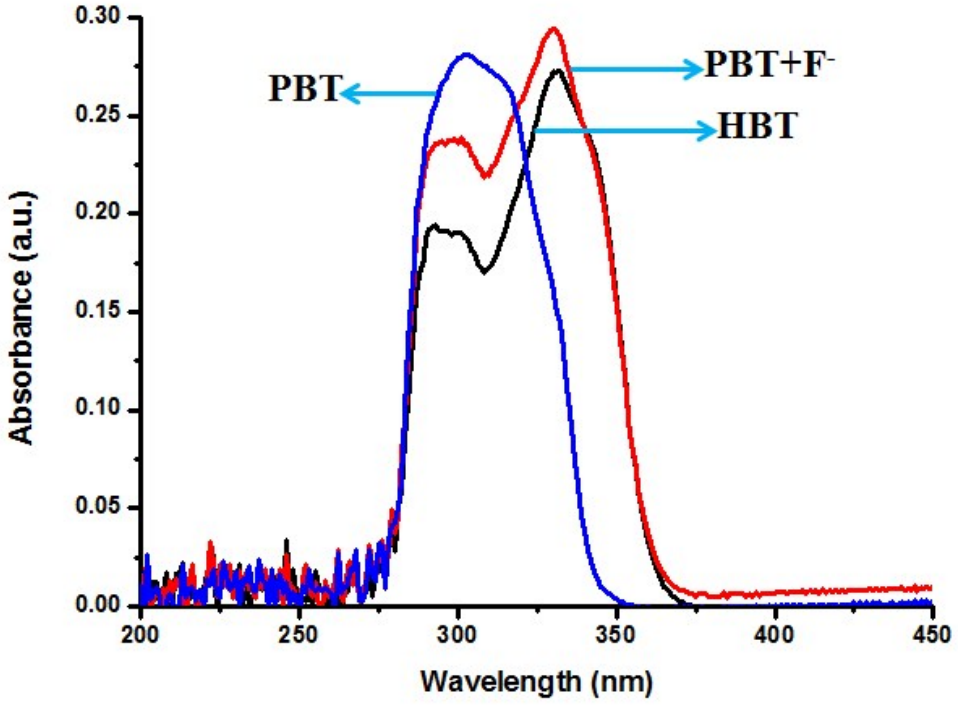

Fig. S3. UV-vis spectra of **PBT** in the absence and presence of F^-. [**PBT** is 10 μM], [F^- is 20 μM] in a mixture of THF and Tris buffer solution (pH 8.0), (1 : 9, v / v).

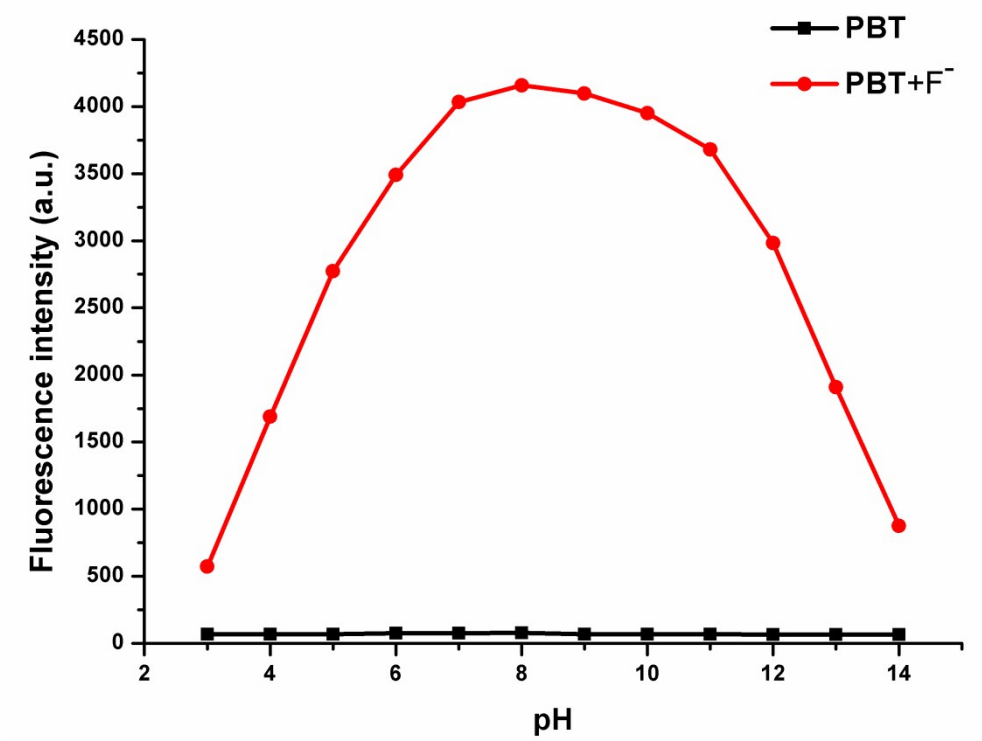

Fig. S4. Effect of pH on the Fluorescence intensity of **PBT** in the absence and presence of F^-. [**PBT** is 10 μM], [F^- is 20 μM] in a mixture of THF and buffer solution (1 : 9, v / v, 25 °C), λ_{ex}=335 nm, λ_{em}=470 nm.

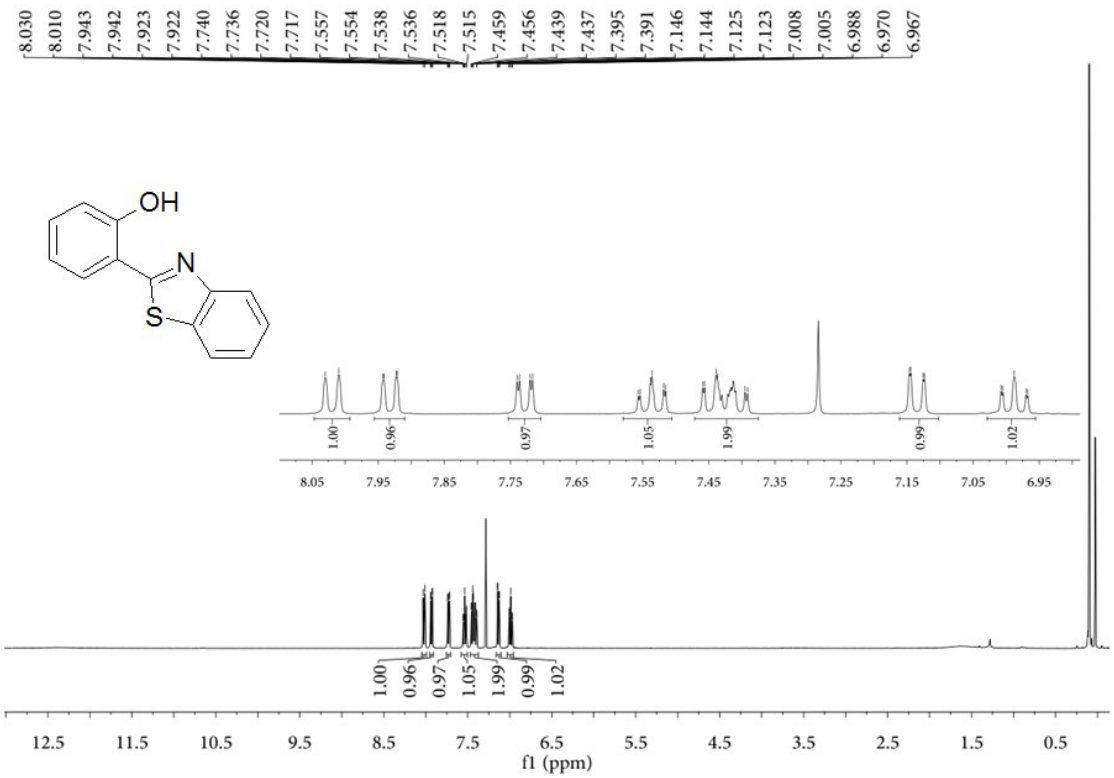

Fig. S5. ^{1}H NMR spectrum of compound **HBT** in $CDCl_3$-d_1.

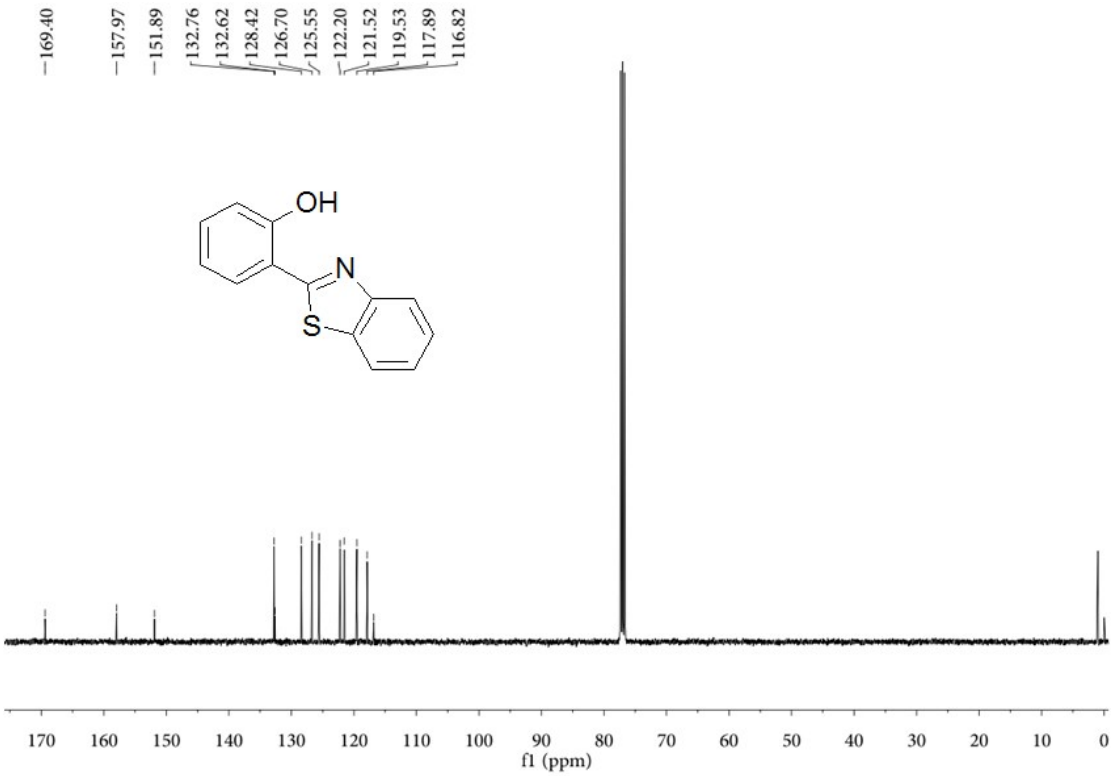

Fig. S6. ^{13}C NMR spectrum of compound **HBT** in $CDCl_3$-d_1.

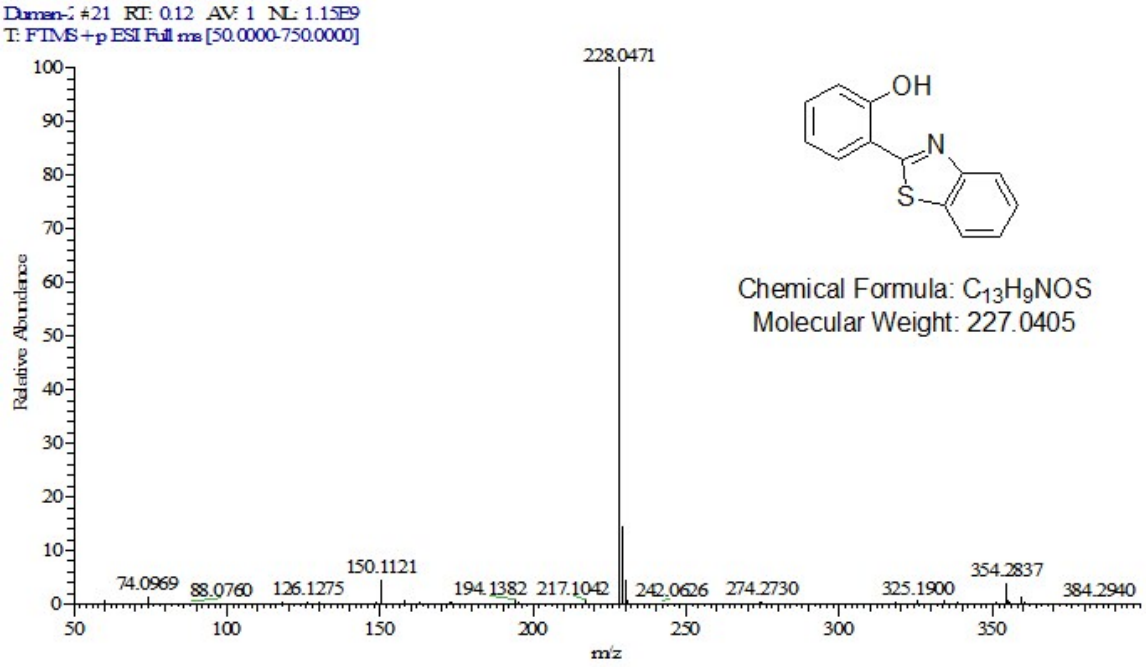

Fig. S7. HRMS spectrum of compound **HBT** in CH_3CN.

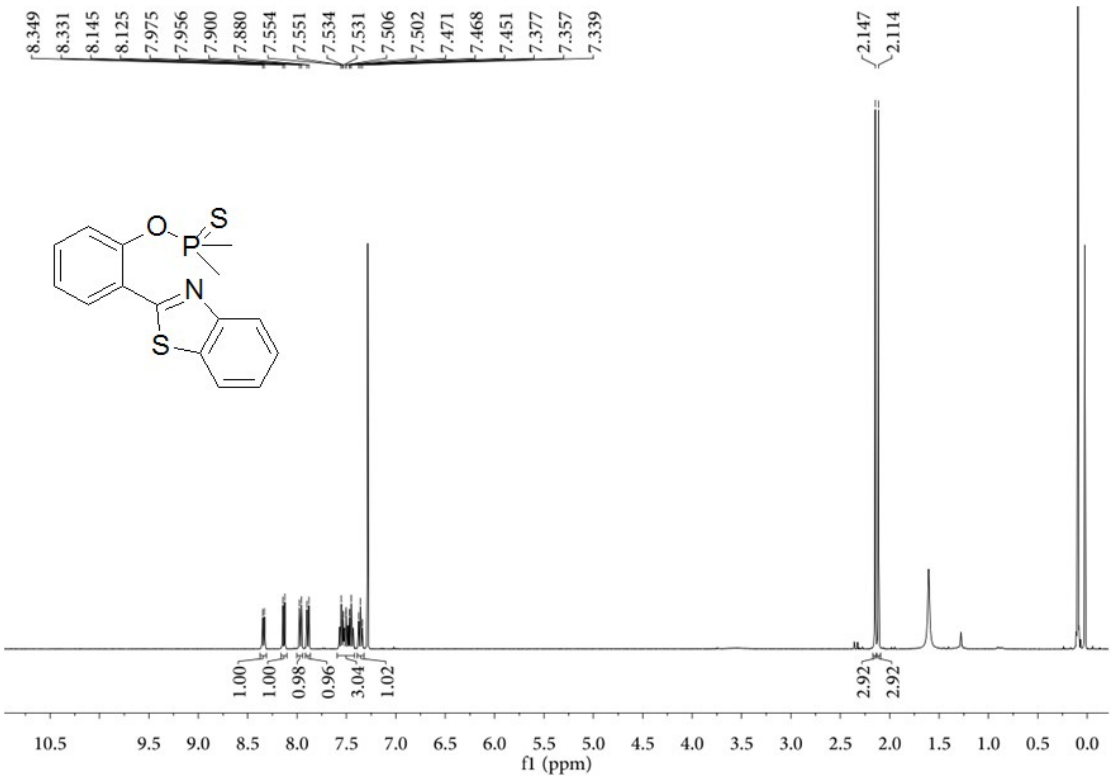

Fig. S8. ^1H NMR spectrum of compound **PBT** in $CDCl_3$-d_1.

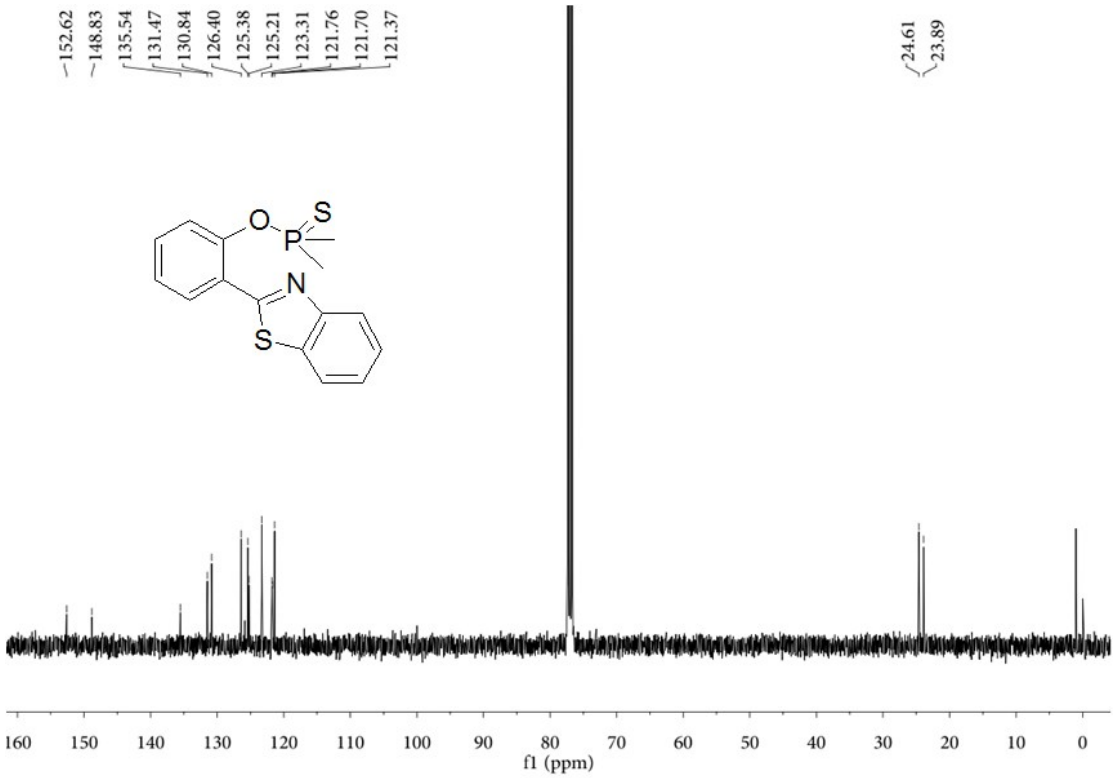

Fig. S9. ^{13}C NMR spectrum of compound **PBT** in $CDCl_3$-d_1.

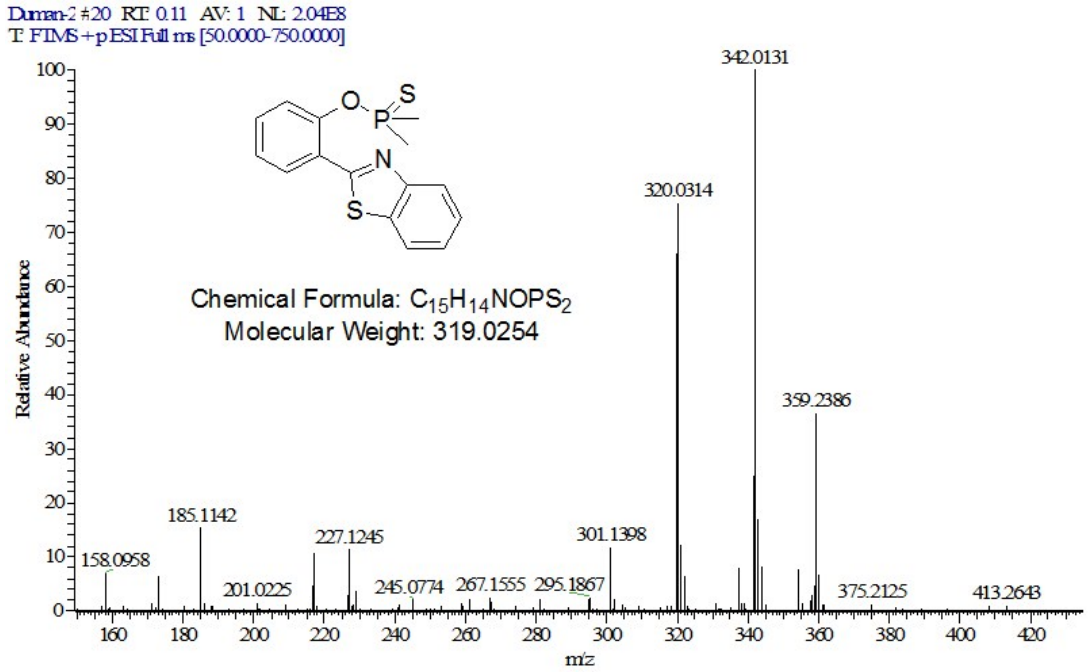

Fig. S10. HRMS spectrum of probe compound **PBT** in CH_3CN.

Detection limit

The detection limit for F^- ions was calculated by the fluorescence titration experiments according to the reported method. A good linear relationship between the fluorescence intensity and F^- concentration (0.5 μM-10 μM) could be obtained (R^2=0.9995). The value obtained for the F^- was found to be 3.8 nM by the equation of $L_{OD}=3\delta/m$ (δ was the standard deviation of the blank solution and m is the absolute value of the slope between intensity versus F^- concentration). δ= 0.4880, m= 389.7332.

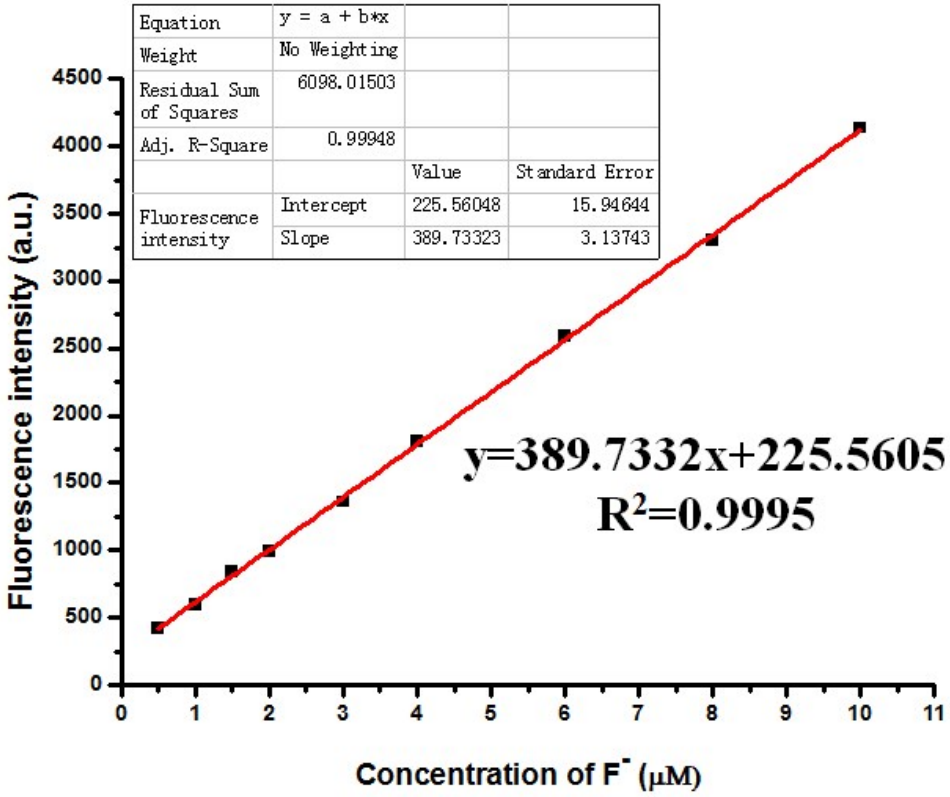

Fig. S11. The linear relationship between the fluorescence intensity and F^- concentration (0.5-10 μM). All measurements were taken in a mixture of THF and Tris buffer solution (pH 8.0), (1 : 9, v / v) at 25 °C. λ_{ex}=335 nm, λ_{em}=470 nm.

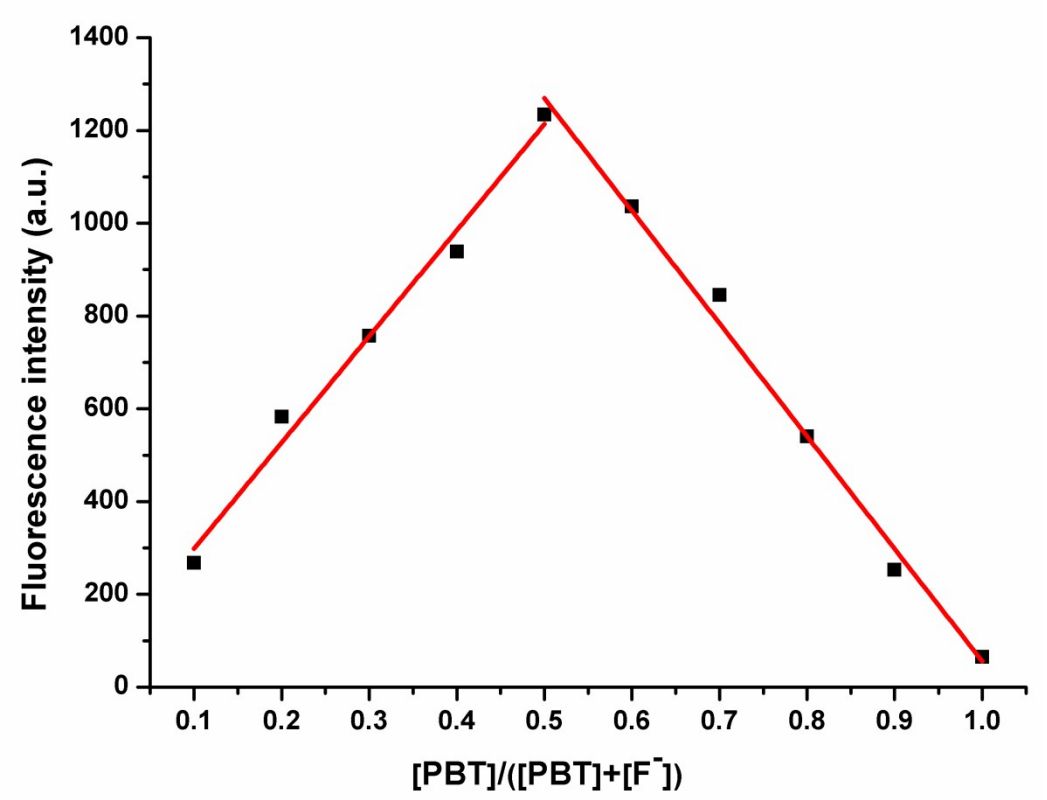

Fig. S12. Job's plot for determining the stoichiometry of **PBT** and F^-. The total concentration of **PBT** and F^- was 10 μM in a mixture of THF and Tris buffer solution (pH 8.0), (1 : 9, v / v) at 25 °C. λ_{ex}=335 nm, λ_{em}=470 nm.

Kinetic studies:

The reaction of **PBT** (10 μM) with F^- in THF (pH 8.0, 90 % Tris-HCl) was monitored using the fluorescence intensity at 470 nm. The reaction was carried out at 25 °C. The *pseudo*-first-order rate constant for the reaction was determined by fitting the fluorescence intensities of the samples to the *pseudo*-first-order equation:

$$\text{Ln}\,[(F_t - F_{min}) / F_{min}] = - k't$$

Where F_t and F_{min} are the fluorescence intensities at 470 nm at time t and the maximum value obtained after the reaction was complete. *k'* is the *pseudo*-first-order rate constant. The *pseudo*-first-order plots for the reaction of **PBT** with 2 equiv. of F^- is shown in Fig. S13, the *pseudo*-first-order rate constant $k' = 1/t_1 = 0.01269\ \text{min}^{-1}$.

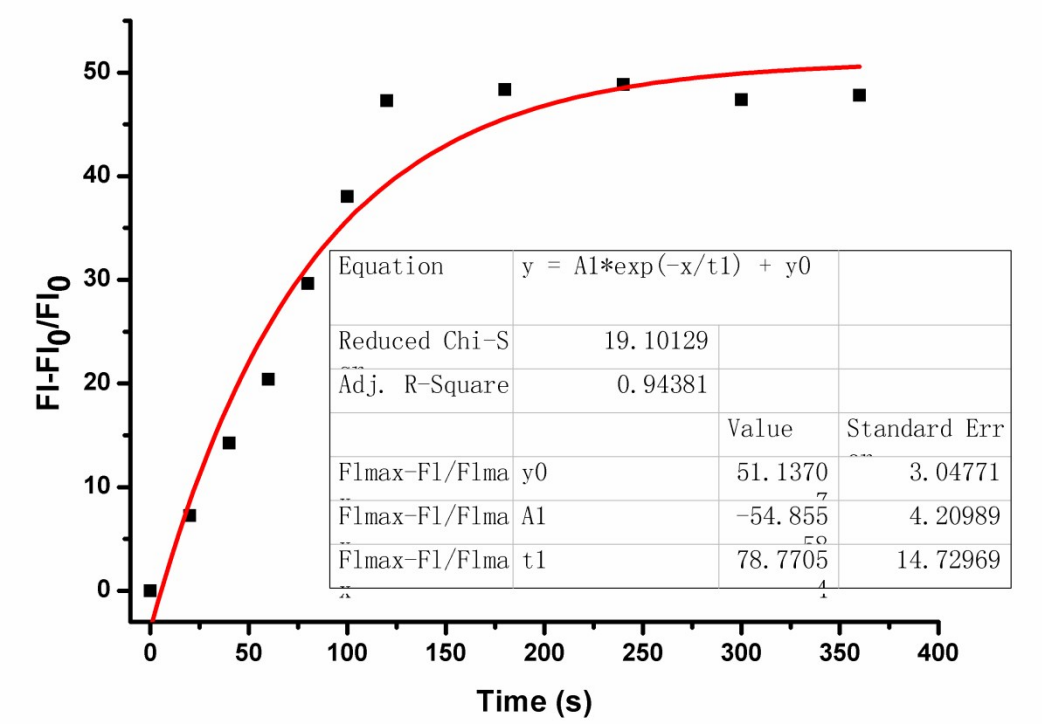

Fig. S13. *Pseudo*-first-order kinetic plot of the reaction of **PBT** (10 μM) with F^- (2 equiv.) a mixture of THF and Tris buffer solution (pH 8.0), (1 : 9, v / v) at 25 °C. $k = 0.01269\ \text{min}^{-1}$.

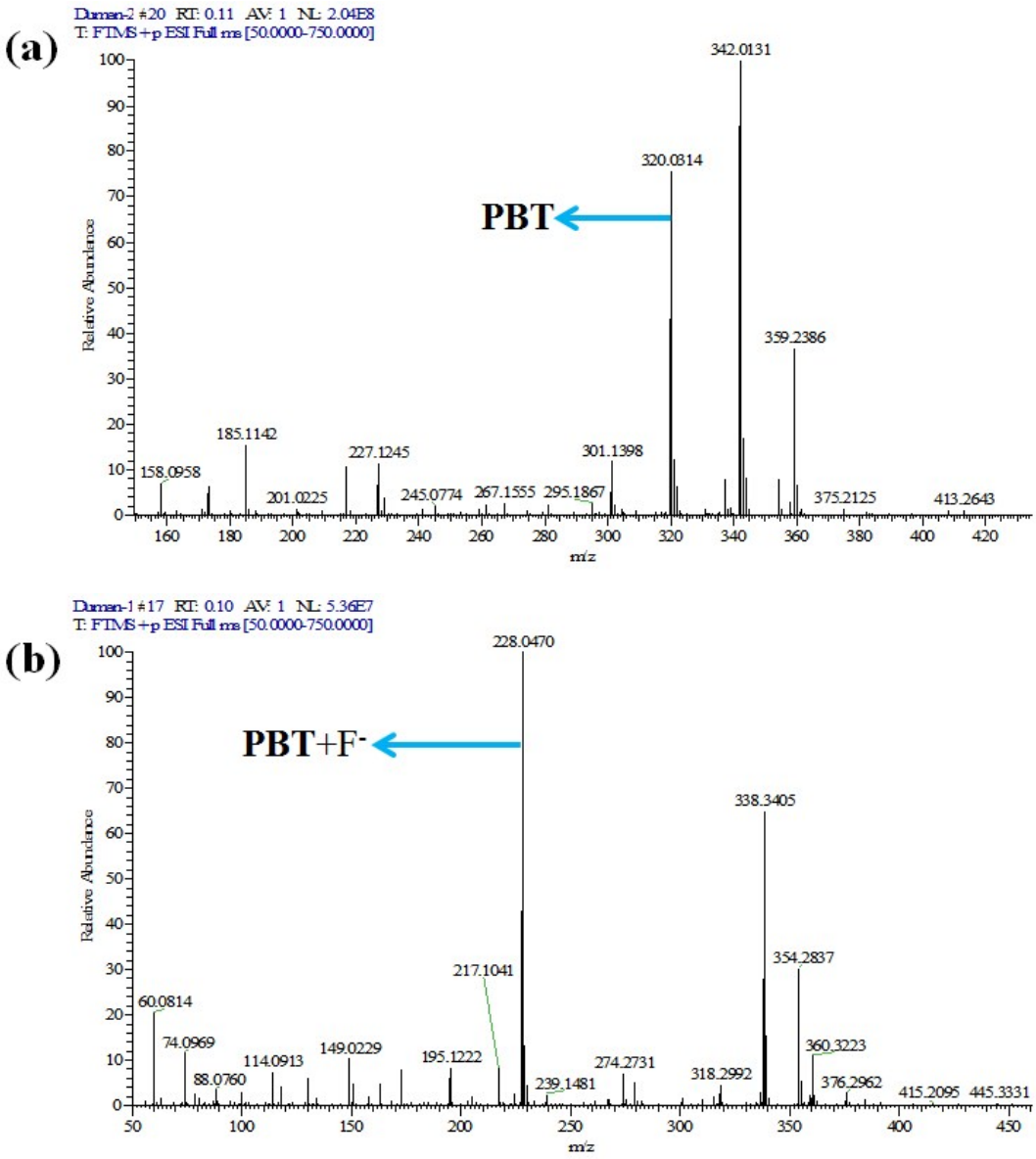

Fig. S14. ESI-MS spectrum (positive ion mode) of **PBT** upon addition of F^- in CH_3CN. (a) only **PBT**, (b) the isolated aggregates of compound after **PBT** reacted with F^- for 10 min.

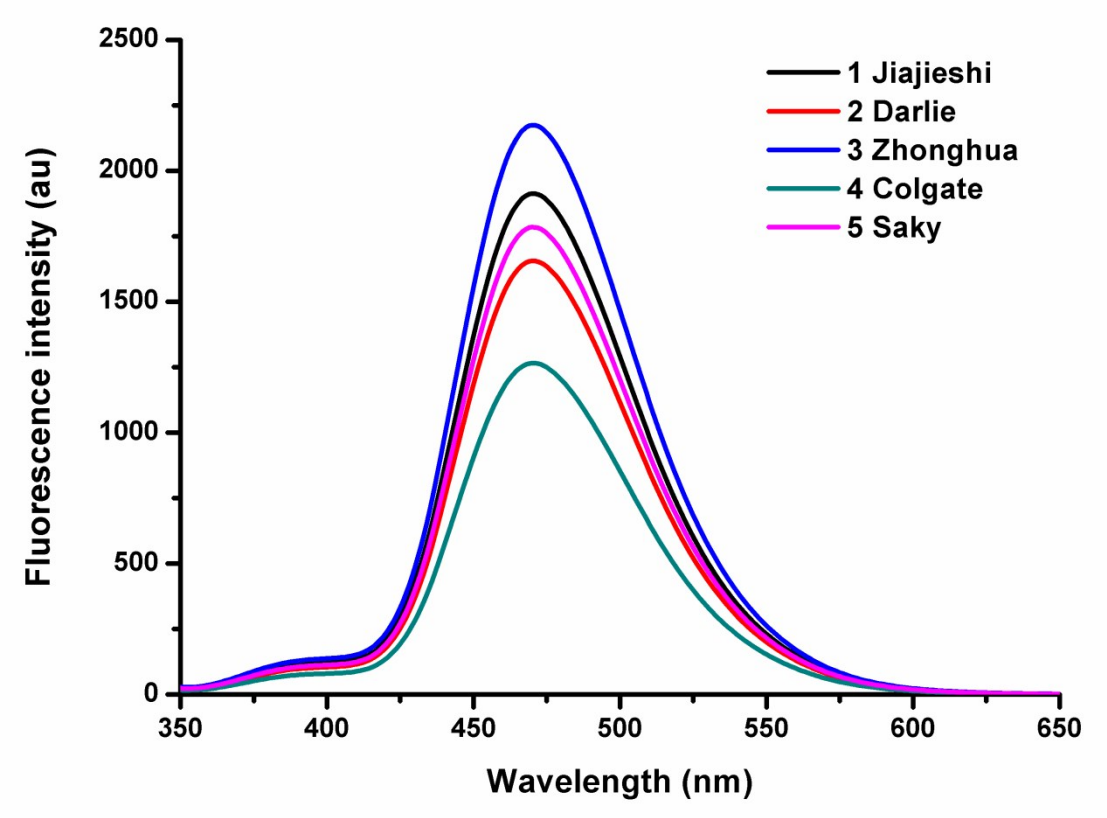

Fig. S15. The fluorescence spectra change of **PBT** upon addition of F^- from toothpastes 1, 2, 3, 4, 5 and 6. λ_{ex}=335 nm, λ_{em}=470 nm.

References

[1] H. Y. Kim, H. G. Im and S. K. Chang, *Dyes and Pigments*, 2015, **112**, 170-175.

[2] X. X. Chen, T. H. Leng, C. Y. Wang , Y. J. Shen and W. H. Zhu, *Dyes and Pigments*, 2017, **141**, 299-305.

[3] M. Bineci, M. Baglan and S. Atılgan, *Sensors and Actuators B*, 2016, **222**, 315-319.

[4] B. W. Ke, W. X. Wu, L. Wei, F. B. Wu, G. Chen, G. He and M. Y. Li, *Anal. Chem.*, 2015, **87**, 9110-9113.

[5] Y. M. Shen, X. Y. Zhang, Y. Y. Zhang, H. T. Li and Y. D. Chen, *Sens. Actuators, B*, 2018, **258**, 544-549.

[6] L. Fu, F. F. Wang, T. Gao, R. Huang, H. He, F. L. Jiang and Y. Liu, *Sens. Actuators, B*, 2015, **216**, 558-562.

[7] X. L. Yu, L. L. Yang, T. T. Zhao, R. L. Zhang, L. Yang, C. L. Jiang, J. Zhao, B. H Liu and Z. P Zhang, *RSC Adv.*, 2017, **7**, 53379-53384.

[8] E. S. Luis, O. T. Adrian, K. Y. Anatoly and P. L. Georgina, *Anal. Lett.*, 2016, **49**, 2301-2311.

[9] M. M. Yu, J. Xu, C. Peng, Z. X. Li, C. X. Liu and L. H. Wei, *Tetrahedron*, 2016, **72**, 273-278.

[10] X. J. Zheng, W. C. Zhu, H. Ai, Y. Huang and Z. Y. Lu, *Tetrahedron Lett.*, 2016, **57**, 5846-5849.

[11] J. Tao, P. Zhao, Y. H. Li, W. J. Zhao, Y. Xiao and R. H. Yang, *Anal. Chim. Acta*, 2016, **918**, 97-102.

[12] Shweta, A. Kumar, Neeraj, S. K. Asthana and K. K. Upadhyay, *New J. Chem.*, 2017, **41**, 5098-5104.

[13] Y. J. Li, Q. Sun, L. Su, L. L. Yang, J. Zhang, L. Yang, B. H. Liu, C. L. Jiang and Z. P. Zhang, *RSC Adv.*, 2018, **8**, 8688-8693.